AIAA 82-4062

A New Solution Method for Lifting Surfaces in Subsonic Flow

T. Ueda* and E. H. Dowell†
Princeton University, Princeton, N. J.

A simple method for calculating the unsteady aerodynamic loadings on harmonically oscillating thin wings in subsonic flow has been developed. The method is based on a concept of concentrated lift forces. The wing is divided into the element surfaces on which lift distributions are represented by single concentrated lift forces. Since the procedure does not include any quadratures, it can be applied easily to calculate the unsteady aerodynamic loadings on complex planform wings even when they have partial span control surfaces. Numerical calculations are carried out for various wing geometries and compared with other analyses and experiments.

Nomenclature

$\mathcal{R}$	= aspect ratio of a wing
B, B_R, B_I	= functions defined by Eqs. (9) and (10)
b	= semichord length of a root chord
C_L, C_ℓ	= complex lift coefficient
C_M, C_m	= complex moment coefficient
D	= matrix defined by Eq. (12)
h	= nondimensional vertical displacement amplitude of a wing
K	= kernel function
k	= reduced frequency
M	= Mach number of a uniform flow
N_x	= chordwise number of elements
N_y	= one-half of the spanwise number of elements
Δp	= nondimensional amplitude of pressure differential
p	= pressure vector
Q	= reduction matrix
R	= parameter defined by Eq. (7)
r	= nondimensional spanwise distance
S	= total wing area
u	= velocity of a uniform flow
w	= nondimensional amplitude of upwash velocity
w	= upwash vector
X	= parameter defined by Eq. (8)
x_0	= parameter defined by Eq. (4)
y_0	= parameter defined by Eq. (5)
α	= angle of attack of a wing
β	= $\sqrt{1-M^2}$
γ	= Euler's constant
Δ_i	= area of an element surface
δ	= flap deflection angle
Φ	= modal matrix
ϕ	= phase angle of complex coefficients
Λ	= sweeping angle of a quarter chord line of a wing
λ	= taper ratio of a wing
σ, σ_i	= one-half width of an element surface
ρ_∞	= air density of a uniform flow

Subscripts

I	= imaginary part
i	= ith element surface
L, ℓ	= lift forces
M, m	= moment forces
R	= real part

Received Jan. 27, 1981; revision received June 8, 1981.

*Research Associate (on leave from National Aerospace Laboratory, Japan). Member AIAA.

†Professor, Dept. of Mechanical and Aerospace Engineering. Associate Fellow AIAA.

Introduction

AN important problem for aeroelasticians[1] is to evaluate the pressure distribution on a wing in oscillatory motion. Many methods[2-7] have been developed for calculating the unsteady pressure distribution on a thin finite wing in subsonic flow since Küssner[8] formulated the governing integral equation in 1940. The methods can be divided into two principal categories, the mode function method[2-4] and the discrete element method.[5-7] Watkins et al.[2] developed the former for practical use. Further developing this method, Rowe et al.[4] calculated successfully the unsteady pressure distribution on wings with control surfaces. However, control surfaces which generate discontinuities in the upwash distribution, and other complex planform configurations, make this procedure sensitive to the manner of representing the additional singularities associated with such geometries.

A typical procedure of the discrete-element method type is the doublet lattice method,[6] which is an extension of the vortex lattice method[9] originally developed for steady flow to the unsteady flow case. This method is used widely (e.g., see Ref. 10) because of its ready applicability to complex wing configurations. Although the method yields reasonable results, it contains an inconsistency in that the steady-state part (the portion independent of the reduced frequency) must be calculated with the aid of the vortex lattice method despite the fact that the basic equation of doublets is valid even when the flow becomes steady.[6] This inconsistency is due to the difficulty in evaluating an improper integral along a spanwise coordinate which one encounters when using the acceleration doublet formulation.

The doublet, which is closely related to the vortex, may be derived purely mathematically as a derivative of the Green function for the Helmholtz equation. Since the kernel function of Küssner's integral equation was derived from the doublet of the acceleration potential which satisfies the same partial differential equation as the velocity potential, it concerns only the pressure differential. On the other hand, the trailing vortex itself makes no contribution to the pressure differential but affects only the upwash distribution. Thus, the upwash induced between the two trailing lines of the horseshoe vortex is hidden in the r^{-2} singularity of the kernel, where r is the spanwise variable defined later by Eq. (6). This is the reason why the singular integral must be evaluated in Mangler's sense.[11]

Since the governing differential equation of the flow becomes the Laplace equation if the flow is steady and/or incompressible, a line of the acceleration doublet can be interpreted directly as the vortex in that case. For an incompressible flow, Jordan[7] evaluated the improper integral accurately using a constant doublet line at a quarter chord of the element.

In the present method, we account for this integration properly, for *compressible, unsteady* flow, not by resorting to the doublet line or the vortex but according to the sense of Mangler in a discrete system. The method, which has the above-mentioned consistency to the steady flow, is much simpler than the doublet lattice method. The wing is divided into segments of small panels and the lifts of individual segments are represented by single concentrated forces which correspond to the acceleration doublet points mathematically. Since no quadrature is required in the procedure, it requires a relatively small amount of computational time. Above all, the method is simple.

The authors found, after they fully developed the method, that a concept similar to the present method has been described independently by Houbolt.[12] His concept, however, did not reach a final result including numerical evaluation for three-dimensional flow which is accomplished by the present paper. Moreover, a key point of the present work is an analytical evaluation[13] of the pressure kernel function.

Some mention should also be made of the so-called panel method. Instead of using Küssner's integral equation, Morino and Kuo[14] adopted a more general form of the integral equation for unsteady flow which includes the Green function of the velocity potential. This panel method has been developed to a higher approximation by Dusto et al.[15] Although the method can be applied to the thickness and body/wing interaction problem as well, Küssner's equation is still essential as far as the circulatory part of the pressure distribution is concerned.

Doublet Point Method

Amplitudes of pressure distributions of oscillatory lifting surfaces and of their upwash velocity are related by the integral equation[1,8] as,

$$w(x,y) = \frac{1}{8\pi} \int \int_{Ra} \Delta p(\xi,\eta) K(x_0,y_0)\, d\xi d\eta \tag{1}$$

The lifting surface is assumed to lie in the plane $z=0$. The symbol Ra denotes the region of the wing area. We treat every quantity of Eq. (1) as a nondimensional value. The semichord length b of the root chord is chosen for nondimensionalizing length variables and the uniform flow speed u for the disturbance velocity. The pressure coefficient Δp is defined by

$$\Delta p = -\frac{p'_+ - p'_-}{\frac{1}{2}\rho_\infty u^2} \tag{2}$$

where p'_+ and p'_- are disturbance pressure of the upper and lower surfaces of a wing, respectively. The denominator in the right-hand side of Eq. (2) is the dynamic pressure of the uniform flow. The kernel function $K(x_0,y_0)$ in Eq. (1) can be written as

$$K(x_0,y_0) = e^{-ikx_0}\left[\frac{Me^{ikX}}{R\sqrt{X^2+r^2}} + B(k,r,X)\right] \tag{3}$$

In Eq. (3), the following parameters have been defined

$$x_0 = x - \xi \tag{4}$$

$$y_0 = y - \eta \tag{5}$$

$$r = |y_0| \tag{6}$$

$$R = \sqrt{x_0^2 + \beta^2 r^2} \tag{7}$$

$$X = (x_0 - MR)/\beta^2 \tag{8}$$

The function $B(k,r,X)$ in the kernel represents an integral function of complex values, i.e.,

$$B(k,r,X) = \int_{-\infty}^{X} \frac{e^{ikv}}{(v^2+r^2)^{3/2}} dv \tag{9}$$

This function can be separated into two real functions as

$$B(k,r,X) = B_R(k,r,X) + i \cdot B_I(k,r,X) \tag{10}$$

Values of these functions can easily be obtained by the series found in Ref. 13. The series is also shown in the Appendix. Since the kernel function $K(x_0,y_0)$ corresponds to a normal velocity field that is produced by a point doublet of the acceleration potential located at (ξ,η), we call the point (ξ,η) a doublet point. Further, we call the point (x,y) an upwash point where the normal velocity of the upwash is placed. Analogous to the doublet lattice method, the wing planform is divided into panel segments called element surfaces. Each element surface is constructed such that the two side edges are parallel to the uniform flow. We identify the individual elements by numbering them from 1 to N (see Fig. 1). As shown in Fig. 2, let us focus our attention on the ith element surface.

The trapezoid of the element has the area Δ_i and the width $2\sigma_i$. Although there is no rigorous verification, following successful application to the doublet lattice method, we adopt the ¼-¾ chord rule[9] for element surfaces. Namely, the lift distribution on the surface is concentrated at the point (ξ_i,η_i) on the quarter chord at the midspan of the element. This is the equivalent to putting there a doublet source of the strength, $\Delta p(\xi_i,\eta_i)\Delta_i$. Thus, the location (ξ_i,η_i) is the doublet point of the element surface. Similarly, the upwash of the three-quarter chord point (x_i,y_i) at midspan is taken as representative for the whole upwash distribution on an element surface. These assumptions make it possible to discretize the integral equation (1) into linear algebraic equations. Instead of Eq. (1), the upwash w_i of the ith element can be calculated in a discrete system by

$$w_i = \frac{1}{8\pi} \sum_{j=1}^{N} \Delta p(\xi_j,\eta_j)\Delta_j \cdot K(x_i-\xi_j, y_i-\eta_j), \quad (i=1\ldots N) \tag{11}$$

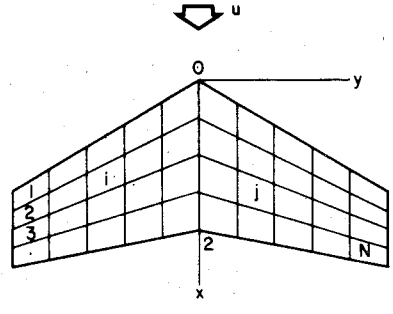

Fig. 1 Element surfaces.

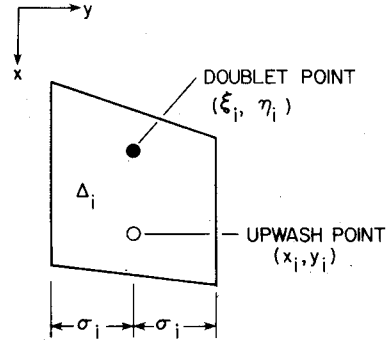

Fig. 2 The *i*th element surface.

If we put

$$D=[d_{ij}]=\frac{\Delta_j}{8\pi}K(x_i-\xi_j,y_i-\eta_j) \tag{12}$$

$$p=\{p_j\}=\{\Delta p(\xi_j,\eta_j)\} \tag{13}$$

$$w=\{w_i\}=\{w(x_i,y_i)\} \tag{14}$$

then, the following algebraic equation is obtained

$$w=Dp \tag{15}$$

The upwash vector w is calculated from the given oscillatory mode shape $h(x,y)$ by

$$w_i=\frac{\partial}{\partial x}h(x_i,y_i)+ikh(x_i,y_i) \tag{16}$$

This is the outline of the discretization. Some mention should be made of the Kutta condition and the singularities of the kernel function. With respect to the Kutta condition at the trailing edge, the ¼-¾ chord rule allows one to avoid imposing directly the Kutta condition on the pressure distribution as is also the case for the doublet lattice method and the vortex lattice method. The singularities, however, require rather careful handling with respect to their discretization. The integral of Eq. (1) has no meaning in an ordinary sense since it becomes infinite because of the r^{-2} singularity in the part of $B_R(k,r,X)$ as $r\to 0$ and $X>0$. If the integration includes this region, we must calculate the integral in Mangler's sense.[11] In order to do this for the discrete system of Eq. (11), we first consider the spanwise integration of the function B_R for the region $r<\sigma$, $X>0$, where the upwash point lies behind the doublet point. The definition due to Mangler is introduced,

$$\oint_{-\sigma}^{\sigma}B_R(k,r,X)\,dy_0=\lim_{\epsilon\to 0}\left[\int_{-\sigma}^{-\epsilon}+\int_{\epsilon}^{\sigma}B_R(k,r,X)\,dy_0-\frac{4}{\epsilon}\right] \quad (X>0) \tag{17}$$

If we utilize the equations,

$$\int_{-\infty}^{-\epsilon}+\int_{\epsilon}^{\infty}\frac{2}{r^2}dy_0=\frac{4}{\epsilon} \tag{18}$$

$$\lim_{\epsilon\to 0}\int_{-\epsilon}^{\epsilon}\left[B_R(k,r,X)-\frac{2}{r^2}\right]dy_0=0 \qquad (X>0) \tag{19}$$

then the definition of Eq. (17) becomes

$$\oint_{-\sigma}^{\sigma}B_R(k,r,X)\,dy_0=\int_{-\sigma}^{\sigma}\left[B_R(k,r,X)-\frac{2}{r^2}\right]dy_0-\frac{4}{\sigma} \quad (X>0) \tag{20}$$

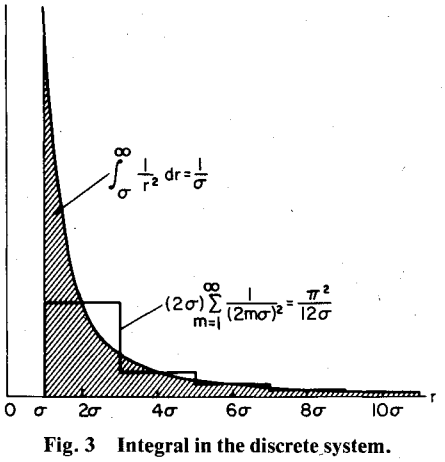

Fig. 3 Integral in the discrete system.

The integral in the right-hand side of Eq. (20) is no longer infinite and has a finite value in the ordinary sense. The function B_R of the positive argument X can be related to that of negative X by means of the modified Bessel function of the second kind as

$$B_R(k,r,X)=-B_R(k,r,-X)+2(k/r)K_1(kr), \quad (X>0) \tag{21}$$

Substitution of Eq. (21) into Eq. (20) and using term-by-term integration yield

$$\oint_{-\sigma}^{\sigma}B_R(k,r,X)\,dy_0=-\int_{-\sigma}^{\sigma}B_R(k,r,-X)\,dy_0-\frac{4}{\sigma}+4k\sum_{n=0}^{\infty}\frac{(k\sigma/2)^{2n+1}}{n!\,(n+1)!\,(2n+1)}\left[\ell n\frac{k\sigma}{2}+\gamma-\sum_{m=1}^{n}\frac{1}{m}-\frac{4n+3}{2(2n+1)\,(n+1)}\right], \quad (X>0) \tag{22}$$

Then, if $k\sigma\ll 1$, the integral can be approximated by

$$\oint_{-\sigma}^{\sigma}B_R(k,r,X)\,dy_0\simeq\int_{-\sigma}^{\sigma}\left[-B_R(k,r,-X)-\frac{2}{\sigma^2}+k^2\left(\ell n\frac{k\sigma}{2}+\gamma-\frac{3}{2}\right)\right]dy_0 \tag{23}$$

It can be seen from Eq. (23) that in order to include the effect of Mangler's integral in a discrete system, the value of the function B_R in the kernel should be replaced by

$$B_R(k,r,X)\to -B_R(k,0,-X)-\frac{2}{\sigma_j^2}+k^2\left(\ell n\frac{k\sigma_j}{2}+\gamma-\frac{3}{2}\right) \tag{24}$$

if the upwash point is located downstream of the doublet point $(\xi_j,\ y_j)$ within a width which is defined by $2\sigma_j$. The second term in the right-hand side of Eq. (24) represents the effect of a horseshoe vortex in the vortex lattice method. It, however, overestimates the effect in a discrete system as it stands. In Eq. (20), the corresponding term can be regarded as cancelling the quantity,

$$2\int_{\sigma}^{\infty}\frac{2}{r^2}dr=\frac{4}{\sigma} \tag{25}$$

On the other hand, in the discrete system, the integral in the left-hand side of Eq. (25) may be evaluated by (see Fig. 3)

$$2(2\sigma)\sum_{m=1}^{\infty}\frac{2}{(2m\sigma)^2}=\frac{\pi^2}{12}\frac{4}{\sigma} \tag{26}$$

This leads us to the conclusion that when an upwash point is downstream of a doublet point, the value of the function B_R should be evaluated by

$$B_R(k,r,X)\to -B_R(k,0,-X)-\frac{\pi^2}{6\sigma_j^2}+k^2\left(\ell n\frac{k\sigma_j}{2}+\gamma-\frac{3}{2}\right) \quad (r<\sigma_j,\ X>0) \tag{27}$$

Although the last term in the right-hand side of Eq. (27) may be expected to have a similar modification, it can be neglected when $k\sigma$ is small.

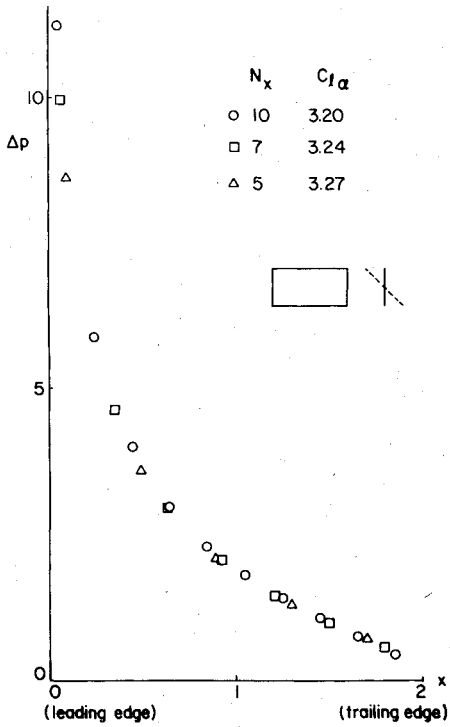

Fig. 4a Dependency on chordwise number of elements N_x ($\mathcal{R}=2$, $k=0$, $M=0$, $N_y=5$, $y=0.2$, $\Lambda=0$ deg, $\lambda=1$).

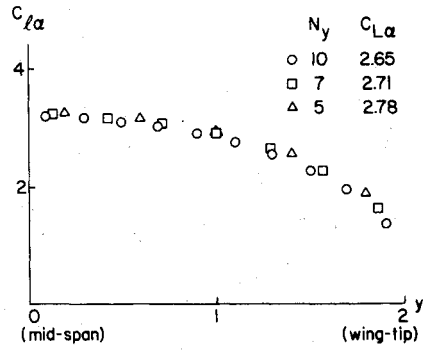

Fig. 4b Dependency on spanwise number of elements N_y ($\mathcal{R}=2$, $k=0$, $M=0$, $N_x=5$, $\Lambda=0$ deg, $\lambda=1$).

Reduction in the Degrees of Freedom

It is efficient to perform a reduction in the number of degrees of freedom before solving the matrix equation of Eq. (15). For example, one may be able to put some constraint on the pressure distribution p by symmetry. In this case, the pressure distribution will be represented by a smaller number of degrees of freedom as

$$p=Q\tilde{p} \tag{28}$$

Then, within the framework of Eq. (28), Eq. (15) can be solved as

$$\tilde{p}=[Q^TDQ]^{-1}Q^Tw \tag{29}$$

Furthermore, if we adopt the modal approach to the discrete system of w so that

$$w=\Phi\tilde{w} \tag{30}$$

then the pressure distribution becomes

$$\tilde{p}=[Q^TDQ]^{-1}Q^T\Phi\tilde{w} \tag{31}$$

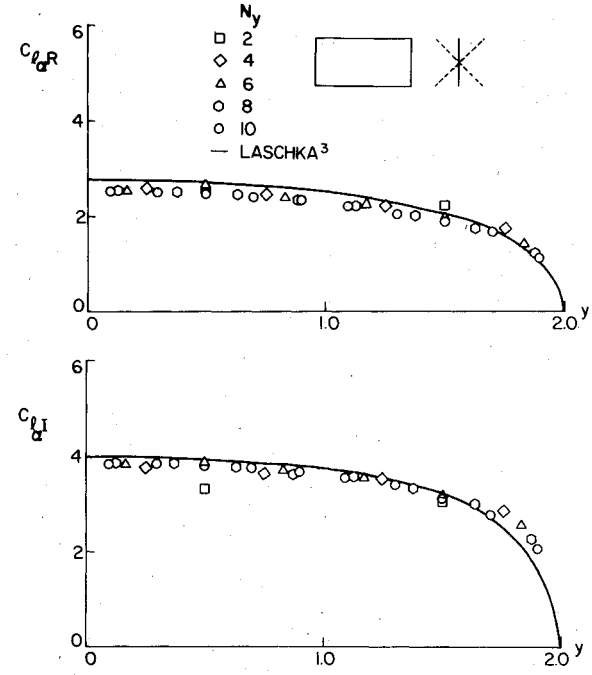

Fig. 5 Dependency on spanwise number of elements in unsteady case ($\mathcal{R}=2$, $k=1$, $M=0$, $N_x=5$, $\Lambda=0$ deg, $\lambda=1$).

Numerical Results

Solving Eq. (15) or Eq. (31), we can directly obtain the pressure differentials which are the concentrated forces at the doublet point divided by the corresponding element area. Although the following definitions are not essential to this method, for convenience we define the complex lift and moment coefficients as

$$C_\ell(y_j)=\sum_i^{N_x}\Delta p_i\Delta_i \Big/ \sum_i^{N_x}\Delta_i \tag{32}$$

(summation is chordwise at $y=y_j$)

$$C_m(y_j)=\sum_i^{N_x}\Delta p_i\Delta_i(x_m-x_i) \Big/ \sum_i^{N_x}\Delta_i \tag{33}$$

(summation is chordwise at $y=y_j$)

$$C_L=\sum_j^{N_y}\left\{C_\ell(y_j)\sum_i^{N_x}\Delta_i\right\} \Big/ (S/2) \tag{34}$$

$$C_M=\sum_j^{N_y}\left\{C_m(y_j)\sum_i^{N_x}\Delta_i\right\} \Big/ (S/2) \tag{35}$$

where S is a total wing area and x_m the location of the axis around which the moment force is to be calculated.

When the reduced frequency tends to zero, the flow becomes steady. For a rectangular wing of $\mathcal{R}$ 2 in steady flow, the pressure distributions and the lift coefficient slopes have been calculated for various numbers of elements as shown in Fig. 4. The chordwise pressure distributions at the location of $y=0.2$ are shown in Fig. 4a for three different chordwise numbers of elements N_x. The spanwise number of elements is fixed at five. It can be seen from the figure that even a small number of elements gives satisfactory results. The convergence in spanwise number of elements is shown in Fig. 4b with a fixed chordwise number of elements. Although the fewer spanwise elements give slightly higher values of the local lift coefficient slope than the values given by the large number of elements especially near the wing tip, it appears relatively insensitive to the number of elements. This property

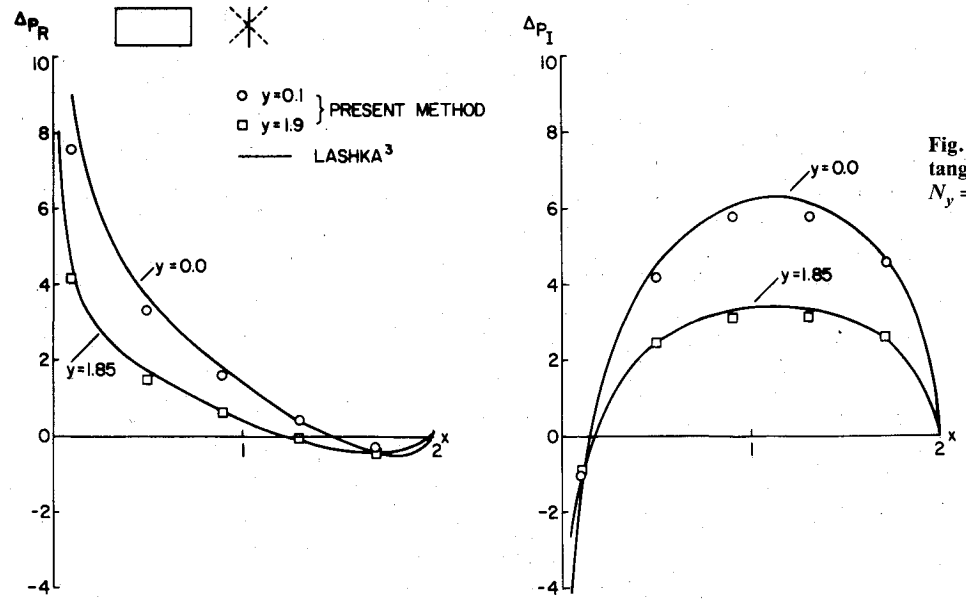

Fig. 6 Pressure distributions of a rectangular wing ($\mathcal{R}=2$, $k=1$, $M=0$, $N_x=5$, $N_y=10$, $\Lambda=0$ deg, $\lambda=1$).

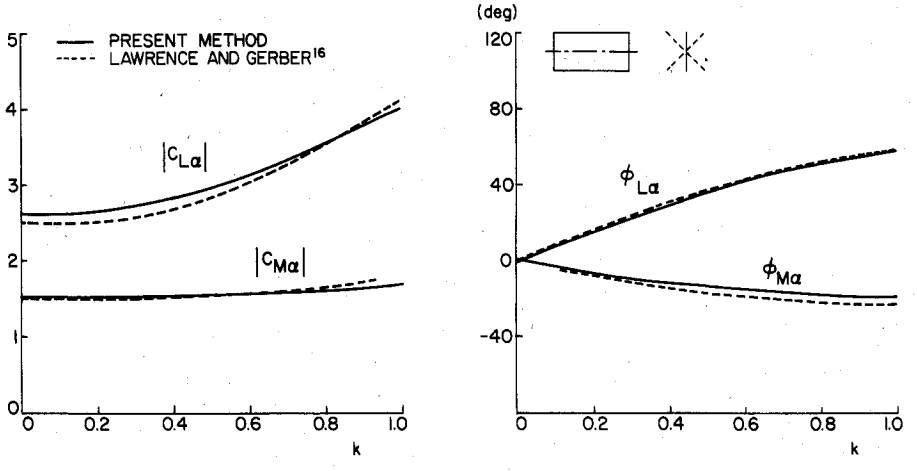

Fig. 7 Lift and moment coefficients vs reduced frequency ($\mathcal{R}=2$, $M=0$, $N_x=5$, $N_y=10$, $\Lambda=0$ deg, $\lambda=1$).

remains as the flow becomes unsteady. Figure 5 depicts the dependency on the spanwise number of elements of the same rectangular wing that oscillates in pitching motion around its midchord axis. The results are compared with those of Laschka[3] which were calculated by the mode function method. Four spanwise elements provide a well-converged solution. If we compare the results for the total lift coefficient, even two spanwise elements give favorable value of $C_L=2.4+3.2i$ while for the 10 spanwise elements the total lift coefficient is $C_L=2.1+3.4i$. Chordwise pressure distributions of 10 spanwise and 5 chordwise elements at two different spanwise locations are shown in Fig. 6 being compared with the results of the mode function method.[3] Both real and imaginary parts of the pressure distributions by the present method are smaller at the inside of the wing and slightly larger near the wing tip than those by the mode function method. This tendency is also seen in Fig. 5. The total lift and moment coefficients of this pitching wing in incompressible flow are compared with the calculation by Lawrence and Gerber[16] for various reduced frequencies in Fig. 7. The agreement between the two results is good.

Calculations have been carried out on two different planform wings which appeared in Ref. 3. The results are compared with those by Laschka[3] in Figs. 8 and 9. The wing shown in Fig. 8 has a sweep angle of 45 deg and oscillates in heaving motion with a unit amplitude. The local moment coefficient in the figure is taken about a point of midlocal chord. Compressibility is also included in this case. Comparison between the two results is satisfactory both for incompressible and compressible flow except for the moment phase angles which exhibit slight differences on the inner span. Figure 9 shows the results for a delta wing of $\mathcal{R}$ 4 which undergoes a pitching motion around the axis penetrating a midchord point at the wing root. The abscissa is reduced frequency. Both the total lift and moment coefficients show good agreement with those of Laschka. In this calculation, 49 element surfaces are used. The average CPU time for computation for one reduced frequency was 8.5 s on an IBM3033 computer. The computational time of this method is almost independent of the planform configuration, which is a great advantage when the wing configuration becomes complex.

Further calculations have been made on two wings having partial span control surfaces. The result for the wing with a deflected partial flap in steady flow is shown in Fig. 10. The result is compared with that by Rowe[4] showing good agreement in spite of a rather coarse element representation for the present method. For the same wing, the result is also compared with the experimental data[17] at $y=1.4$ in Fig. 11. The chordwise distribution of the experiment was measured at the location of 44% semispan ($y=1.47$). The result by the doublet lattice method[6] using 10 chordwise and 8 spanwise lattice is also depicted in the figure. The pressures on the flap, calculated by both methods, indicate slightly higher values than the experimental data.

The unsteady pressure distribution obtained by the present method is shown in Fig. 12 for the wing having an outboard

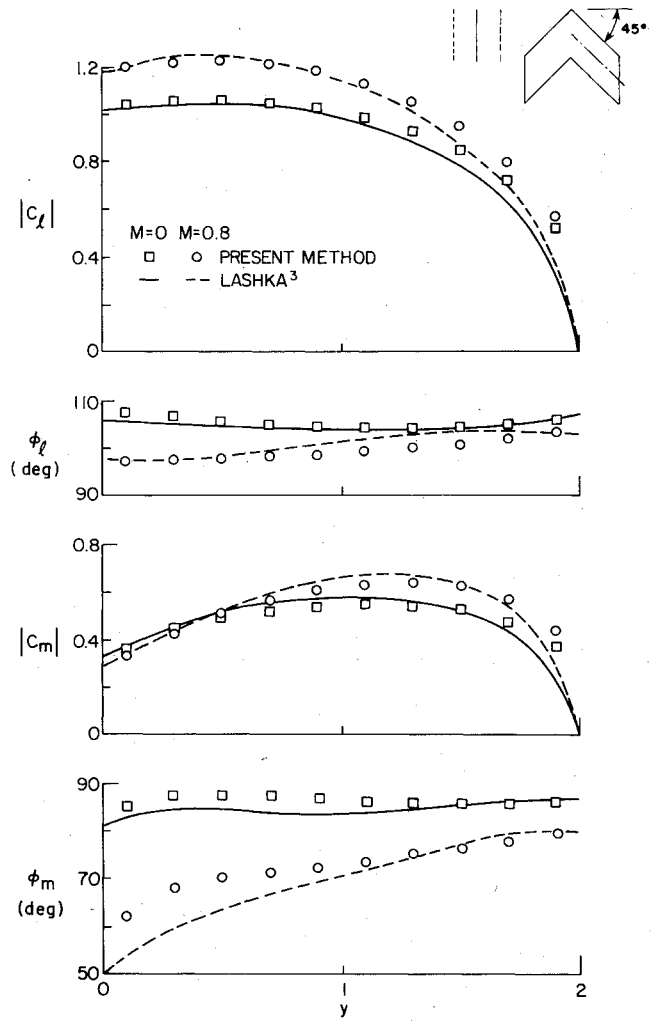

Fig. 8 Local lift and moment coefficients of a sweptback wing ($\mathcal{R}=2$, $k=0.4$, $N_x=5$, $N_y=10$, $\Lambda=45$ deg, $\lambda=1$).

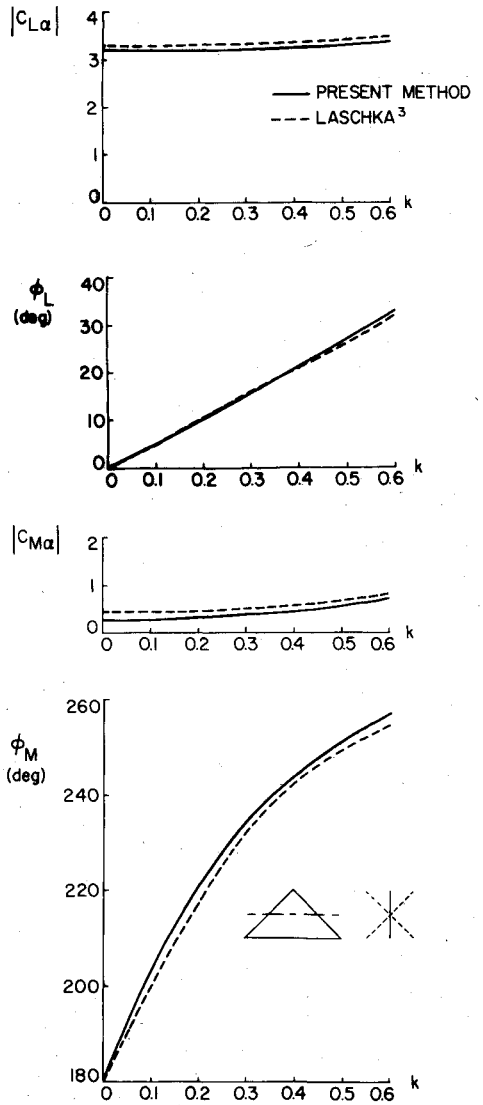

Fig. 9 Lift and moment coefficients of a delta wing ($\mathcal{R}=4$, $M=0$, $N_x=N_y=7$, $\Lambda=36.9$ deg, $\lambda=0$).

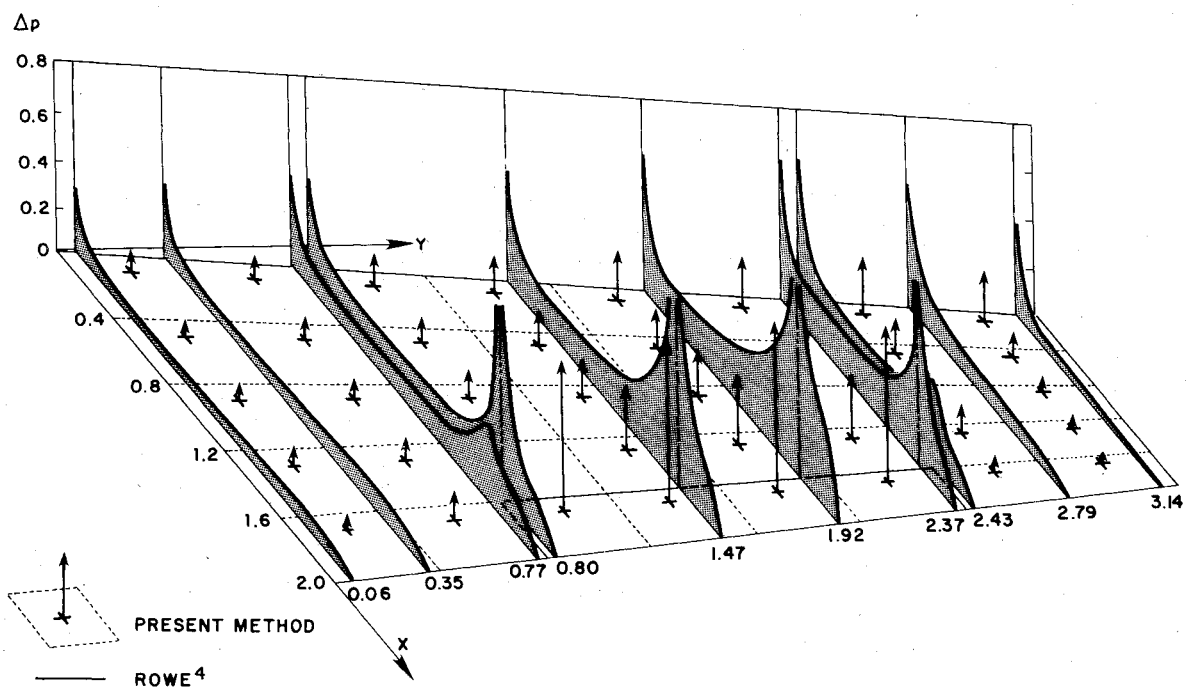

Fig. 10 Pressure distribution of a wing with deflected flap ($\mathcal{R}=4$, $k=0$, $M=0.6$, $N_x=5$, $N_y=8$, $\Lambda=35$ deg, $\lambda=0.6$, $\alpha=0$ deg, $\delta=10$ deg).

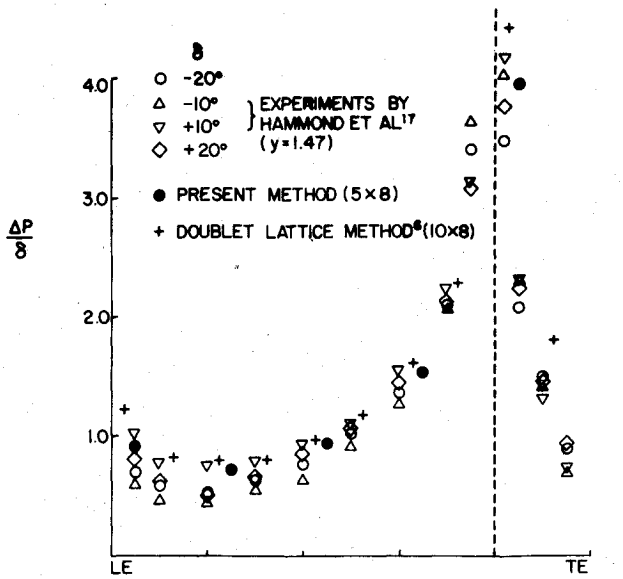

Fig. 11 Comparison with experimental data of the deflected flap wing ($N_x=5$, $N_y=8$, $y=1.4$).

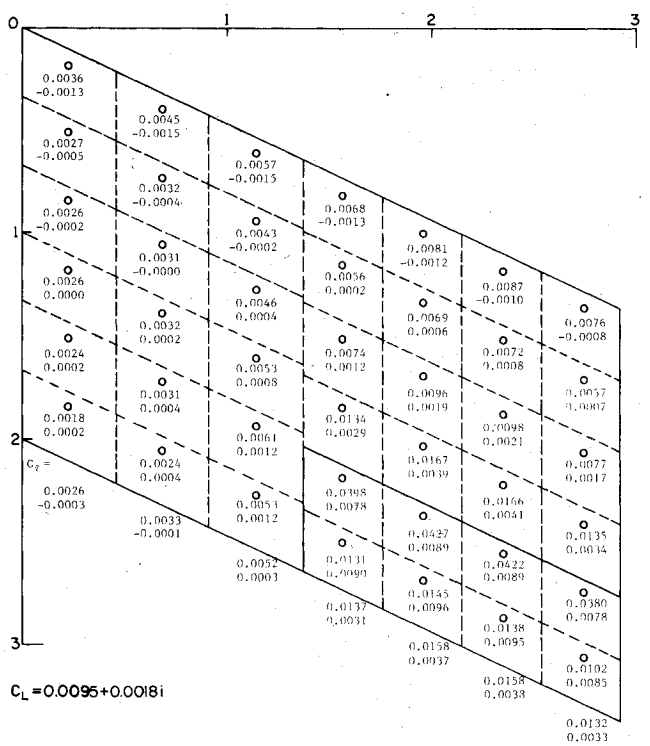

Fig. 12 Results for unsteady pressure distribution of the wing with oscillating partial flap ($\mathcal{R}=2.94$, $k=0.372$, $M=0$, $\Lambda=25$ deg, $\lambda=1$, $\delta=0.66$ deg).

flap which is flapping with an amplitude of 0.66 deg. The flap was divided into eight equal elements in the calculation. The upper and the lower figures written in an element are the in-phase and out-of-phase components of the pressure at the doublet point, respectively. In Fig. 13, the values of the third streamwise row from the wing tip, $y=1.95$, are compared with the experimental results by Försching et al.[18] Although the exact location of the experimental data cannot be found in Ref. 18, the agreement is encouraging if we consider the simplicity of the present method. The computational time for this wing including the steady flow case ($k=0$) was 12.6 s.

Finally, we show the result obtained by the present method for a straight tapered wing which has been proposed as a

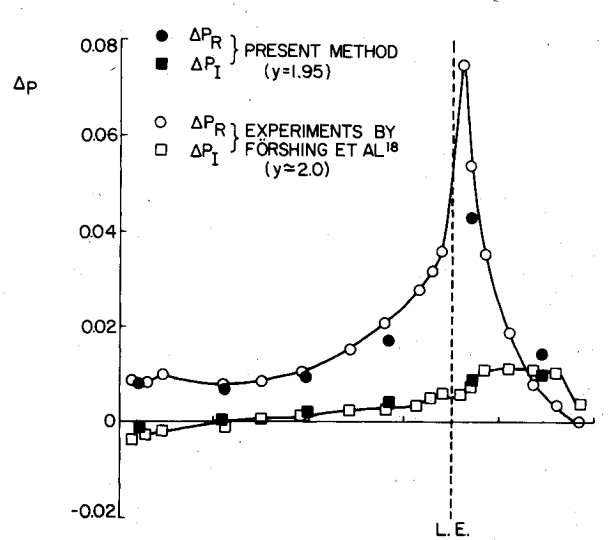

Fig. 13 Comparison with experimental data of the oscillating flap wing.

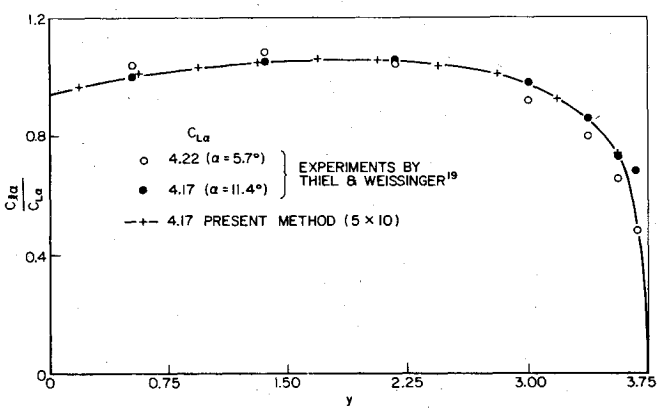

Fig. 14 Local lift-curve slope for a sample wing ($\mathcal{R}=5$, $k=0$, $M=0$, $N_x=5$, $N_y=10$, $\Lambda=0$ deg, $\lambda=0.5$).

sample wing to gain an appreciation for the accuracy of various lifting surface methods.[9] The flow is assumed incompressible and steady. The spanwise distribution of the local lift-curve slope normalized by the global value is shown in Fig. 14 and compared with experimental data obtained by Theil and Weissinger.[19] The agreement between the present method and experiment data is excellent, especially for the pressure distribution measurements at an angle of attack of 11.4 deg.

Conclusion

The doublet point method has been developed for calculating the subsonic unsteady aerodynamic forces which act on two-dimensional wings. The numerical results are promising if one considers that the method is so simple that it is easy to program for computation. Since it is based on a concept of concentrated forces, the results obtained by the present method are readily combined with aeroelastic analyses for flexible wings. For example, the problems of flutter, active flutter suppression, and gust alleviation, separately or together using the finite-element method of structural analysis, may be treated.

Appendix

The real functions in the right-hand side of Eq. (10) are

$$B_R(k,r,X)=\int_{-\infty}^{X}\frac{\cos kv}{(v^2+r^2)^{3/2}}\,dv \qquad \text{(A1)}$$

$$B_1(k,r,X) = \int_{-\infty}^{X} \frac{\sin kv}{(v^2+r^2)^{3/2}}\,dv \tag{A2}$$

These functions can be expanded in series as,

$$B_R(k,r,X) = \sum_{n=0}^{\infty}(-1)^n U_{2n} - \frac{k^2}{2}\sum_{n=0}^{\infty}\frac{(kr/2)^{2n}}{(n+1)(n!)^2} \times\left\{\sum_{m=1}^{n}\frac{1}{m}+\frac{1}{2(n+1)}-\gamma-\ell n\frac{k}{2}\right\} \tag{A3}$$

$$B_I(k,r,X) = \sum_{n=0}^{\infty}(-1)^n U_{2n+1} + \frac{\pi}{4}k^2\sum_{n=0}^{\infty}\frac{(kr/2)^{2n}}{(n+1)(n!)^2} \tag{A4}$$

where the term U_n which is a function of X can be calculated with the aid of the recurrence formula,

$$U_m = \frac{k}{(m-2)m!}\frac{(kX)^{m-1}}{\sqrt{X^2+r^2}} - \frac{(kr)^2}{m(m-2)}U_{m-2} \quad (m\geq 3) \tag{A5}$$

The initial terms of the recurrence formula (A5) are given by

$$U_1 = -k/\sqrt{X^2+r^2} \tag{A6}$$

$$U_2 = -\frac{k^2}{2}\left\{\frac{X}{\sqrt{X^2+r^2}}+\ell n(\sqrt{X^2+r^2}-X)\right\} \tag{A7}$$

Equation (A3) also requires U_0,

$$U_0 = \frac{1}{\sqrt{X^2+r^2}(\sqrt{X^2+r^2}-X)} \tag{A8}$$

Acknowledgments

This work was supported in part by NASA Grant NSG-2194 with the Ames Research Center. The authors would like to thank John C. Houbolt, William P. Rodden, and E. Carson Yates Jr. for stimulating and helpful discussions of the earlier literature.

References

[1] Dowell, E. H. et al., *A Modern Course in Aeroelasticity,* Sijthoff and Noordhoff, Alphen aan den Rijn, The Netherlands, 1978.

[2] Watkins, C. E., Woolston, D. S., and Cunningham, H. J., "A Systematic Kernel Function Procedure for Determining Aerodynamic Forces on Oscillating or Steady Finite Wings at Subsonic Speeds," NASA TR R-48, 1959.

[3] Laschka, B., "Zur Theorie der harmonisch schwingenden tragenden Flache bei Unterschallanstromung," *Zeitschrift für Flugwissenschaften,* Heft 7, 1963, pp. 265-292.

[4] Rowe, W. S., Redman, M. C., Ehlers, F. E., and Sebastian, J. D., "Prediction of Unsteady Aerodynamic Loadings Caused by Leading Edge and Trailing Edge Control Surface Motion in Subsonic Compressible Flow—Analysis and Results," NASA CR-2543, 1975.

[5] Landahl, M. T. and Stark, J. E., "Numerical Lifting-Surface Theory—Problems and Progress," *AIAA Journal,* Vol. 6, Nov. 1968, pp. 2049-2060.

[6] Albano, E. and Rodden, W. P., "A Doublet-Lattice Method for Calculating Lift Distributions on Oscillating Surfaces in Subsonic Flows," *AIAA Journal,* Vol. 7, Feb. 1969, pp. 279-285.

[7] Jordan, P. F., "Reliable Lifting Surface Solutions for Unsteady Flow," *Journal of Aircraft,* Vol. 15, Sept. 1978, pp. 626-633.

[8] Küssner, H. G., "General Airfoil Theory," NACA TM 979, 1941 (also see Luftfahrtforschung, Bd. 17, Lfg. 11/12, 1940, pp. 370-378).

[9] "Vortex-Lattice Utilization," NASA SP-405, 1976.

[10] Ashley, H. and Rodden, W. P., "Wing-Body Aerodynamic Interaction," *Annual Review of Fluid Mechanics,* Vol. 4, 1972, pp. 431-472.

[11] Mangler, K. W., "Improper Integrals in Theoretical Aerodynamics," RAE Rept. Aero. 2424, 1951.

[12] Houbolt, J. C., "Some New Concepts in Oscillatory Lifting Surface Theory," AFFDL-TR-69-2, 1969.

[13] Ueda, T., "Asymptotic Expansion of the Kernel Function in Subsonic Unsteady Lifting Surface Theory," *Journal of Japan Society of Aero/Space Sciences,* Vol. 29, No. 326, 1981, pp. 169-174.

[14] Morino, L. and Kuo, C.-C., "Subsonic Potential Aerodynamics for Complex Configuration: A General Theory," *AIAA Journal,* Vol. 12, Feb. 1974, pp. 191-197.

[15] Dusto, A. R., Epton, M. A., and Johnson, F. T., "Advanced Panel Type Influence Coefficient Methods Applied to Unsteady Three Dimensional Potential Flows," AIAA Paper 78-229, 1978.

[16] Lawrence, H. R. and Gerber, E. H., "The Aerodynamic Forces on Low Aspect Ratio Wings Oscillating in an Incompressible Flow," *Journal of Aeronautical Sciences,* Vol. 19, Nov. 1952, pp. 769-781 (errata issued, Vol. 20, April 1953, p. 296).

[17] Hammond, A. D. and Keffer, B. M., "The Effect at High Subsonic Speeds of a Flap-Type Aileron on the Chordwise Pressure Distribution Near Midsemispan of a Tapered 35° Sweptback Wing of Aspect Ratio 4 Having NACA 65A006 Airfoil Section," NACA RM L53C23, 1953.

[18] Försching, H., Triebstein, H., and Wagener, J., "Pressure Measurements on an Harmonically Oscillating Swept Wing with Two Control Surfaces in Incompressible Flow," *Symposium on Unsteady Aerodynamics for Aeroelastic Analyses of Interfering Surfaces,* AGARD-CP-80-71, Pt. II, 1971, pp. 15-2—15-12.

[19] Theil, A. and Weissinger, J., "Pressure-Distribution Measurements on a Straight and on a 35° Swept-Back Tapered Wing," NACA TM 1126, 1947 (translated from Deutsche Versuchsanstalt für Luftfahrt, Institut für Aerodynamik, Deutsche Luftfahrtforschung, Untersuchungen und Mitteilungen, No. 1293, Sept. 29, 1944).